THE JOURNAL OF BIOLOGICAL CHEMISTRY VOL. 282, NO. ??, pp. 1–xxx, ???? ??, 2007

Membrane-permeable Calmodulin Inhibitors (*e.g.* W-7/W-13) Bind to Membranes, Changing the Electrostatic Surface Potential

*DUAL EFFECT OF W-13 ON EPIDERMAL GROWTH FACTOR RECEPTOR ACTIVATION**

Received for publication, July 28, 2006, and in revised form, December 15, 2006 Published, JBC Papers in Press, January 16, 2007, DOI 10.1074/jbc.M607211200

Parijat Sengupta[‡], María José Ruano[§], Francesc Tebar[¶1], Urszula Golebiewska[‡], Irina Zaitseva[‡], Carlos Enrich[¶], Stuart McLaughlin[‡2], and Antonio Villalobo[§3]

From the [‡]Department of Physiology and Biophysics, Health Science Center, State University of New York at Stony Brook, Stony Brook, New York 11794-8661, [§]Instituto de Investigaciones Biomédicas, Consejo Superior de Investigaciones Científica and Universidad Autónoma de Madrid, Arturo Duperier 4, Madrid E-28029, Spain, and the [¶]Departament de Biologia Cellular i Anatomia Patològica, Universitat de Barcelona, Facultat de Medicina, Casanova 143, Barcelona E-08036, Spain

Membrane-permeable calmodulin inhibitors, such as the napthalenesulfonamide derivatives W-7/W-13, trifluoperazine, and calmidazolium, are used widely to investigate the role of calcium/calmodulin (Ca^{2+}/CaM) in living cells. If two chemically different inhibitors (*e.g.* W-7 and trifluoperazine) produce similar effects, investigators often assume the effects are due to CaM inhibition. Zeta potential measurements, however, show that these amphipathic weak bases bind to phospholipid vesicles at the same concentrations as they inhibit Ca^{2+}/CaM; this suggests that they also bind to the inner leaflet of the plasma membrane, reducing its negative electrostatic surface potential. This change will cause electrostatically bound clusters of basic residues on peripheral (*e.g.* Src and K-Ras4B) and integral (*e.g.* epidermal growth factor receptor (EGFR)) proteins to translocate from the membrane to the cytoplasm. We measured inhibitor-mediated translocation of a simple basic peptide corresponding to the calmodulin-binding juxtamembrane region of the EGFR on model membranes; W-7/W-13 causes translocation of this peptide from membrane to solution, suggesting that caution must be exercised when interpreting the results obtained with these inhibitors in living cells. We present evidence that they exert dual effects on autophosphorylation of EGFR; W-13 *inhibits* epidermal growth factor-dependent EGFR autophosphorylation under different experimental conditions, but in the absence of epidermal growth factor, W-13 *stimulates* autophosphorylation of the receptor in four different cell types. Our interpretation is that the former effect is due to W-13 inhibition of Ca^{2+}/CaM, but the latter results could be due to binding of W-13 to the plasma membrane.

The ubiquitous second messenger Ca^{2+} (1, 2) exerts many of its signaling effects by binding to calmodulin (CaM)[4]; Ca^{2+}/calmodulin (Ca^{2+}/CaM) in turn binds to and modulates the function of >100 target proteins (3–6). Many investigators have used membrane-permeable calmodulin inhibitors (*e.g.* trifluoperazine (TFP), calmidazolium (CDZ), and the napthalenesulfonamide derivatives W-7/W-13) to sort out the multiple potential roles of calmodulin in living cells; a PubMed search for W-7 alone turns up 1,700 publications. Frequently, investigators reason that if two or more chemically distinct inhibitors (*e.g.* W-7 and TFP) produce similar effects on a cell, they can assume that the effects are due to specific inhibition of calmodulin. If, however, these amphipathic weak bases bind to Ca^{2+}/CaM mainly through *nonspecific* hydrophobic and electrostatic interactions, they also will bind to the inner leaflet of the plasma membrane at about the same concentration at which they inhibit calmodulin. This binding reduces the net negative charge on the inner leaflet, which is due mainly to the monovalent acidic lipid 1-palmitoyl-2-oleoyl-*sn*-glycero-3-phosphatidylserine (PS). Decreasing the net negative charge on the inner

* This work was supported by National Institutes of Health Grant GM24971 and a grant from the Baldwin Foundation (to S. M.); Dirección General de Investigación, Ministerio de Educación y Ciencia Grant SAF2005-00631, Fondo de Investigaciones Sanitarias Grant RTICCC C03/10, and European Commission Grant MCRTN-CT-2005-019561 (to A. V.); Ministerio de Educación y Ciencia Grants BMC2003-04754 and GEN2003-20662) (to C. E.); and Ministerio de Educación y Ciencia Grant BMC2003-09496 (to F. T.). The costs of publication of this article were defrayed in part by the payment of page charges. This article must therefore be hereby marked "*advertisement*" in accordance with 18 U.S.C. Section 1734 solely to indicate this fact.

[S] The on-line version of this article (available at http://www.jbc.org) contains supplemental Fig. S1.

[1] Supported by the Ramón y Cajal research Program, Ministerio de Educación y Ciencia (Spain).

[2] To whom correspondence may be addressed: Dept. of Physiology and Biophysics, Health Science Center, State University of New York at Stony Brook, Stony Brook, NY 11794-8661. Tel.: 631-444-3615; Fax: 631-444-3432; E-mail: Stuart.McLaughlin@stonybrook.edu.

[3] To whom correspondence may be addressed: Instituto de Investigaciones Biomédicas, Consejo Superior de Investigaciones Científica and Universidad Autónoma de Madrid, Arturo Duperier 4, E-28029 Madrid, Spain. Tel.: 34-91-585-4424; Fax: 34-91-585-4401; E-mail: antonio.villalobo@iib.uam.es.

[4] The abbreviations and trivial names used are: CaM, calmodulin; CDZ, calmidazolium; EGF, epidermal growth factor; EGFR, EGF receptor; FCS, fluorescence correlation spectroscopy; GF109203X, 3-4-(1H-indol-3-yl)1H-pyrrole-2,5-dione; GFP, green fluorescent protein; HPLC, high performance liquid chromatography; KN-93, 2-[*N*-(2-hydroxyethyl)]-*N*-(4-methoxybenzenesulfonyl)] amino-*N*-(4-chlorocinnamyl)-*N*-methylbenzylamine); JM, juxtamembrane; LUV, large unilamellar vesicle; MALDI-TOF, matrix-assisted laser desorption/ionization time-of-flight; MARCKS, myristoylated alanine-rich C kinase substrate; MOPS, 3-(*N*-morpholino)propanesulfonic acid; PC, phosphatidylcholine; PG, phosphatidylglycerol; PS, phosphatidylserine; TFP, trifluoperazine; W-7, *N*-(6-aminohexyl)-5-chloro-1-naphthalenesulfonamide; W-12, *N*-(4-aminobutyl)-1-naphthalenesulfonamide; W-13, *N*-(4-aminobutyl)-5-chloro-1-naphthalenesulfonamide; PAE, porcine aortic endothelial; MLV, multilamellar vesicle.

leaflet of the plasma membrane can have several biological effects. For example, it could reduce the electrostatically mediated (7–10) membrane binding of clusters of basic residues on numerous peripheral (*e.g.* K-Ras4B, Src, myristoylated alanine-rich C kinase substrate (MARCKS), and gravin) and integral proteins (*e.g.* receptor tyrosine kinases, such as the epidermal growth factor receptor (EGFR)).

We investigated whether commonly used membrane-permeable calmodulin inhibitors bind to phospholipid vesicles formed with the same mole fraction of PS present in the inner leaflet of a typical mammalian plasma membrane. They do. For example, ~10 μM W-7 or W-13 reduces the negative zeta potential of a phospholipid vesicle significantly and induces membrane-bound basic peptide translocation from membrane to solution, as determined by both centrifugation and fluorescence correlation spectroscopy (FCS) measurements; the same inhibitor concentration binds to and inhibits Ca^{2+}/CaM.

Our results suggest that these inhibitors bind both to Ca^{2+}/CaM and to membranes in cells. We investigated the dual effects of Ca^{2+}/CaM inhibitors on an important cellular process, EGFR activation. Exposing cells to EGF produces receptor dimerization (11) and a transient increase in the cytoplasmic free concentration of Ca^{2+}, $[Ca^{2+}]_i$, and consequently in Ca^{2+}/CaM (12–17). We hypothesize that this transient increase in Ca^{2+}/CaM could be important in EGFR activation, because Ca^{2+}/CaM binds both to the EGFR (18–20) and to peptides corresponding to its cytoplasmic juxtamembrane (JM; residues 645–660) region with a sufficiently high affinity (K_d ~ 10 nM for the peptide) (21) to suggest that this interaction could be biologically relevant. A recent report provides important evidence that ligand-mediated activation of EGFR involves dimer formation between two kinase domains, which stimulates rearrangement of the activation loop within the kinase domain by an allosteric mechanism (22–24). Ca^{2+}/CaM, for example, could facilitate formation of the kinase domain dimers by enhancing desorption of the JM plus kinase domains from the cytoplasmic leaflet (7, 25).

Previous published (20, 21) and unpublished work showed that treating cells with appropriate concentrations of W-7, W-13, and the less potent W-12 inhibits the initial transient phase of EGF-stimulated intermolecular EGFR autophosphorylation (hereafter referred to as autophosphorylation) in five different cell types. We report new experiments that provide additional evidence that W-13 inhibits this phase of EGF-mediated autophosphorylation by inhibiting Ca^{2+}/CaM in cells exposed to a calcium ionophore. These results support the hypothesis that Ca^{2+}/CaM is involved in the initial phase of ligand-mediated EGFR activation in several cell types. Introducing a mutation that impedes Ca^{2+}/CaM binding to the EGFR JM domain abrogates W-13-mediated inhibition of EGFR autophosphorylation, which suggests that Ca^{2+}/CaM interacts directly with the EGFR.

W-7 and W-13, however, exert an opposing effect that appears *not* to be restricted to their ability to inhibit Ca^{2+}/CaM; measurements on four different cell types show that W-13 *stimulates* autophosphorylation of EGFR in the *absence* of EGF, confirming and extending earlier work (21, 26, 27). We discuss how the membrane binding of W-7 and W-13 could produce this effect.

EXPERIMENTAL PROCEDURES

Electrostatic Potentials Adjacent to Membranes and Determination of the Zeta Potential—Fixed negative charges on the inner leaflet of a typical mammalian plasma membrane are due mainly to the presence of monovalent acidic lipids, such as PS, which accounts for 20–35% of these phospholipids (28). Most other lipids are neutral (*e.g.* cholesterol) or zwitterionic (*e.g.* 1-palmitoyl-2-oleoyl-*sn*-glycero-3-phosphatidylcholine (PC) and phosphatidylethanolamine); positive lipids are rare or absent. The fixed charges on PS (*red circles* at *left* in Fig. 1*A*) attract ions of opposite charge, K^+ (*blue circles*), from the aqueous phase; these counterions form an ion atmosphere, as shown in Fig. 1*A*. Helmholtz in 1879 (29) first recognized that the fixed charges and counterions "form an electrical double layer . . . that has an extraordinarily small, but not disappearing thickness"; double layer theory is discussed in detail in an excellent modern physical chemical text (30) and reviews of membrane electrostatics (*e.g.* Refs. 31 and 32 and references therein). The essential features are summarized very briefly below and in Fig. 1.

The thickness of the ion atmosphere adjacent to the inner leaflet is about 1 nm = 10 Å. The counterions do not stick to the membrane surface for the same reason the gas molecules in the earth's atmosphere do not fall to the ground; they diffuse away from a region of high concentration. Gouy and Chapman used the Poisson equation to describe the electrostatic attraction of the counterions for the charged surface and the Boltzmann equation to describe the statistical distribution of the counter- and co-ions in the aqueous diffuse double layer; Fig. 1, *B* and *C*, illustrates two key predictions of the Gouy-Chapman theory.

When the surface potential, $\psi(0)$, is small, it is proportional to both the surface charge density, σ (number of fixed charges per unit area of surface), and the Debye length,

$$\psi(0) = \sigma/\epsilon_r\epsilon_o\kappa \qquad \text{(Eq. 1)}$$

where ϵ_r is the dielectric constant or relative permittivity (~80), ϵ_o is the permittivity of free space, and $1/\kappa$ is the Debye length (~1 nm for 0.1 M salt; ~10 nm for 0.001 M salt). Note that this limiting form of the Gouy equation also describes the potential difference between two capacitor plates with charge density σ separated by a distance $1/\kappa$ (see Fig. 1*C*). Equation 1 and the simple capacitor model illustrate the following two important features of double layer theory. The surface potential increases with increasing density of fixed charge (*i.e.* fraction of acidic lipids increases) and/or Debye length (*i.e.* salt concentration decreases). Fig. 1*B* shows the dependence of potential on distance. When the potential in the aqueous phase is small, it falls with distance x from the surface according to Equation 2.

$$\psi(x) = \psi(0)\exp(-\kappa x) \qquad \text{(Eq. 2)}$$

Numerous experimental studies have shown that this theory provides a surprisingly accurate description of the potential adjacent to a phospholipid bilayer membrane (32).

The Helmholtz-Smoluchowski equation gives the relationship between the measured electrophoretic mobility, μ (veloc-

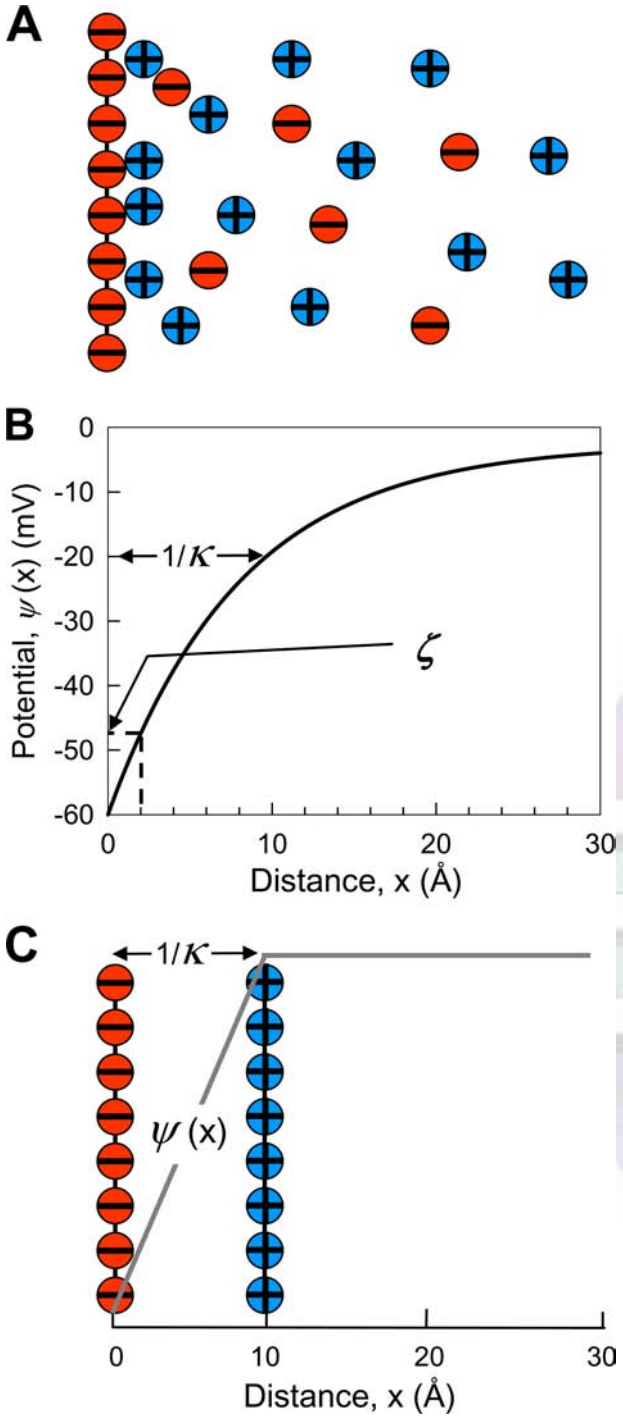

FIGURE 1. **The electrostatic potential adjacent to the inner leaflet of a plasma membrane or a phospholipid bilayer.** *A*, schematic diagram of a surface with fixed negative charges (*e.g.* PS (*red circles* on surface)) that attract ions of opposite charge (*e.g.* K^+ (*blue circles* in solution)); this forms an ionic atmosphere or "diffuse double layer" in the adjacent aqueous phase. *B*, the potential adjacent to the surface falls approximately exponentially with distance. The space constant is the Debye length, $1/\kappa$, which is about 10 Å in a 100 mM salt solution. The potential is drawn according to the Gouy-Chapman theory for a surface with a charge density of one electronic charge per 300 $Å^2$. Experiments show that the zeta potential, ζ, of a phospholipid vesicle is the potential 2 Å from the surface, as indicated in the diagram. *C*, capacitor model of the diffuse double layer. If all of the counterions are located a Debye length from the surface, the fixed charges on the membranes and the counterions in the aqueous phase constitute a parallel plate capacitor, which is a good model of the double layer. Note that decreasing the net number of charges per unit area on the membrane by 50% (*e.g.* by adsorption of a positively charged weak base, such as W-7) also decreases the potential at the surface by 50%.

ity of a multilamellar vesicle in a unit electric field), and the zeta potential, ζ,

$$\zeta = \mu\eta/(\epsilon_r\epsilon_o) \qquad \text{(Eq. 3)}$$

where η is the viscosity of the aqueous solution, ϵ_r is the dielectric constant (~80) and ϵ_o is the permittivity of free space. By definition, ζ is the potential at the hydrodynamic plane of shear, which experiments suggest is located about 0.2 nm from the surface (see Fig. 1*B*) in a 100 mM salt solution (32). The experimental aspects of determining the electrophoretic mobility are considered in detail elsewhere (33). For the experiments shown in Figs. 3 and 4, we added the inhibitor in excess concentration relative to the lipids ([lipid] $< 1\ \mu$M), so the binding of inhibitor to the vesicles does not significantly decrease its free concentration in solution.

Reagents—Fig. 2 shows the chemical structures of five commonly used membrane-permeable calmodulin inhibitors. The naphthalenesulfonamide derivatives (W-7, W-12, and W-13), trifluoperazine (TFP), and calmidazolium (CDZ) are all amphipathic weak bases. (As discussed in the supplemental materials, the neutral form of these weak bases equilibrates between the bathing solution and cytoplasm.) W-7, W-13, and W-12 were purchased from both Sigma and Calbiochem. Similar results (zeta potential and peptide binding to large unilamellar vesicles (LUVs)) were obtained with both samples. CDZ, TFP, and rhodamine green were purchased from Sigma. The phospholipids PC, 1-palmitoyl-2-oleoyl-*sn*-glycero-3-phosphatidylglycerol (PG) and PS were from Avanti Polar Lipids (Alabaster, AL). Peptides corresponding to the JM region of EGFR (EGFR-(645–660)), with and without a Cys residue at the N terminus, were purchased from American Peptide Co. (Sunnyvale, CA). Alexa-488 maleimide was purchased from Invitrogen. Radioactively labeled [*dioleoyl*-1-^{14}C]L-α-dioleoylphosphatidylcholine and [*ethyl*-1,2-^{3}H]*N*-ethylmaleimide were from PerkinElmer Life Sciences.

Cell culture media and sera were purchased from Invitrogen or Biological Industries (Beit Haemek, Israel). Mouse monoclonal anti-phosphotyrosine RC20 antibody conjugated to horseradish peroxidase was from Transduction Laboratories/BD Biosciences. A23187, ionomycin, and KN-93 were from Calbiochem. GF109203X and Fast Green FCF were from Sigma. The enhanced chemiluminescent Luminol (ECL™) reagents were from Amersham Biosciences. Polyvinylidene difluoride membranes were from Pall Gelman Laboratory (Ann Arbor, MI), and Immobilon-P filters were from Millipore Corp. (Billerica, MA).

Vesicle Preparation—We used 100-nm diameter LUVs for the FCS and centrifugation-binding experiments, as described in detail elsewhere (34). Briefly, we added a mixture of solutions of PC and PS in chloroform to a 50-ml round-bottom flask, which was then immersed in a 30–35 °C water bath and attached to a rotary evaporator. The flask was rotated without vacuum for ~5 min to warm the flask and solution. We then evaporated most of the solvent rapidly by applying the maximum vacuum that does not boil the chloroform. The flask was kept under full vacuum for 30 min to remove all traces of chloroform. A solution (typically containing 100 mM KCl, 10 mM

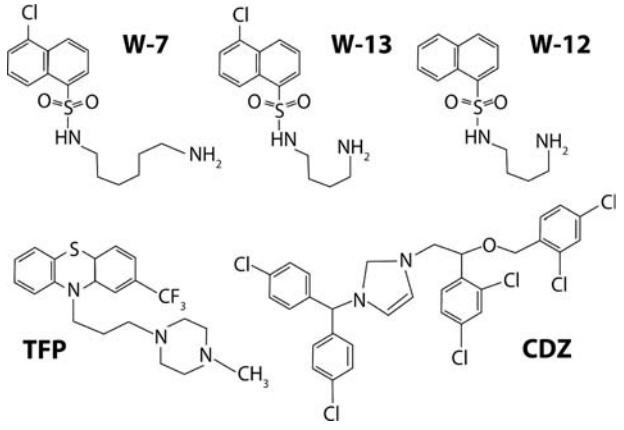

FIGURE 2. **Chemical structures of commonly used membrane-permeable inhibitors of calcium-calmodulin (Ca^{2+}/CaM).** All of these compounds are amphipathic weak bases. *Top line*, naphthalene sulfonamide derivatives, W-7, W-13, and W-12. *Bottom line*, TFP and CDZ. CDZ binds to Ca^{2+}/CaM with a $K_d = 3$ nM (51); TFP with a $K_d = 5$ μM (51, 52); W-7 with reported $K_d = 5$ μM (51), 10 μM (86), and 25 μM (52).

MOPS, pH 7.0) was added to form multilamellar vesicles (MLVs), followed by five cycles of rapid freezing and thawing. We formed LUVs by extruding the MLVs through 100-nm diameter polycarbonate filters. (A solution containing 176 mM sucrose, 10 mM MOPS, pH 7.0, was used to obtain sucrose-loaded LUVs for centrifugation binding measurements. The solution bathing the LUVs was then exchanged for 100 mM KCl, 10 mM MOPS, pH 7.) We used MLVs, which typically had a diameter of 10–20 μm for electrophoretic mobility/zeta potential measurements.

Peptide Labeling and Purification—Labeled or unlabeled peptides used for experiments were determined to be >95% pure by HPLC and MALDI-TOF mass spectroscopy. We used a protocol modified from Ref. 87 to label the peptides with the thiol-reactive fluorescent probes. In brief, we mixed 1 ml of 1 mM peptide in 10 mM K_2HPO_4/KH_2PO_4, pH 7.0, with the probe dissolved in *N*,*N*-dimethyl formamide (probe/peptide molar ratio 1:1) for 1 h. We purified the labeled peptide using HPLC and checked that it has the correct molecular weight using MALDI-TOF mass spectrometry (Proteomics Center, State University of New York at Stony Brook). We labeled the peptides with [*ethyl*-1,2-^{3}H]*N*-ethylmaleimide as described previously (34–36).

Centrifugation Measurements—We measured the binding of EGFR-(645–660) peptides to sucrose-loaded PC/PS LUVs using a centrifugation technique described previously (21, 34, 37). Briefly, sucrose-loaded PC/PS LUVs (20 μM lipid for data in Fig. 5) were mixed with trace concentrations of [*ethyl*-1,2-^{3}H]*N*-ethylmaleimide-labeled peptides (typically 2–10 nM). The mixture was centrifuged at 100,000 × *g* for 1 h. We calculated the percentage of peptide bound by measuring the radioactivity of the peptide in the supernatant and in the pellet.

FCS Measurements and Data Analysis/Interpretation—Information about the size of a particle (*e.g.* free *versus* vesicle-bound peptide) can be obtained by measuring its diffusion constant *D* and using the Stokes-Einstein relationship,

$$D = kT/(6\pi\eta R) \quad \text{(Eq. 4)}$$

where k is the Boltzmann constant, T is the temperature, η is the viscosity of the medium, and R is the hydrodynamic radius of the diffusing particle. We can determine D by measuring the residence time τ_D of a particle diffusing through a small observation volume of radius r and using the Einstein relation for diffusion,

$$r^2 = 4D\tau_D \quad \text{(Eq. 5)}$$

FCS measures the residence time, τ_D of molecules diffusing through a small, optically defined, open probe volume using sensitive fluorescence detection (38–41). Fig. 6 illustrates the principle of FCS and how this technique can be used to measure the binding of fluorescently labeled EGFR-(645–660) to negatively charged phospholipid vesicles (35). Fig. 6*B* shows a schematic diagram of free and LUV-bound peptides undergoing Brownian motion in the laser focus volume; the fluorescence signal from this probe volume fluctuates as the molecules diffuse in and out of it. This fluorescence fluctuation is recorded with an avalanche photodiode detector with good temporal resolution and then analyzed by a digital temporal correlator to compute the autocorrelation function $G(\tau)$, the measured variable for FCS experiments, as described in the supplemental materials. Fig. 6, *C* and *D*, shows the fluorescence time traces and the autocorrelation functions calculated from those time traces, respectively, using the same color coding. We can extract the characteristic residence time, τ_D, of a molecule (*i.e.* the average time the molecule takes to diffuse in and out of the ~300-nm diameter probe volume) by fitting the autocorrelation functions to the appropriate equation. Because the LUV-bound peptides diffuse more slowly than free peptides, the autocorrelation function decays on a longer time scale, and the correlation time is ~25-fold longer. It is easy to distinguish the bound and free species when $\tau_{D(\text{bound})}$ is $\gg \tau_{D(\text{free})}$.

Cell Cultures—N7 × HERc fibroblasts, a stable transfected cell line expressing the wild type human EGFR, was donated by Axel Ullrich from the Max-Planck-Institut für Biochemie (Martinsried, Germany), and RI1 fibroblasts, a stable transfected cell line expressing a human EGFR mutant with an insertion of a highly acidic 23-amino acid sequence between Arg^{647} and His^{648}, which divides the CaM-binding domain into two segments (42), was a kind gift of Andrey Sorokin from the Medical College of Wisconsin (Milwaukee WI). N7 × HERc, N7 × HERc/654A, RI1, EGFR-T17 (stably transfected mouse fibroblasts overexpressing human EGFR), and green monkey kidney COS-1 cells (expressing 4×10^5 EGFR/cell) were grown in Dulbecco's modified Eagle's medium supplemented with 10% (v/v) fetal bovine serum, 5 mM pyruvate, 2 mM L-glutamine, and 40 μg/ml gentamicin in a humidified atmosphere of 5% (v/v) CO_2 at 37 °C. Mouse NIH3T3 (clone WT8) fibroblasts (expressing 4×10^5 EGFRs/cell) (43) were grown as above except that 10% (v/v) donor calf serum was used. Porcine aortic endothelial (PAE/EGFR-GFP) cells, a stable transfected cell line expressing a human EGFR-green fluorescent protein (GFP) chimera (2×10^5 EGFR-GFP/cell) (44), were grown in F-12 medium with the supplements indicated above. Cells were counted using a Neubauer's chamber after detachment from the culture dishes and seeded in 6-well plates (1.4×10^5 cells/well) in the media

indicated above and grown to ~90% confluence for 24 h. Thereafter, the cells were washed twice with phosphate-buffered saline (137 mM NaCl, 2.7 mM KCl, 1.8 mM KH_2PO_4, and 10 mM Na_2HPO_4 at pH 7.4) and maintained overnight in a serum-free medium before performing the experiments.

Measurement of EGFR Autophosphorylation—EGF-dependent EGFR autophosphorylation was measured upon the addition of 10 nM EGF to serum-starved cells in multiwell plates containing 2 ml of medium. Depending on the experiment (see legends to Figs. 7 and S1), the medium also contained a calcium/calmodulin-activated kinase II inhibitor, a protein kinase C inhibitor, the CaM inhibitor W-13, and a Ca^{2+} ionophore. We added 1 ml of ice-cold 30% trichloroacetic acid to stop the reaction and prepared a total cell lysate using Laemmli sample buffer, boiling the sample for 5 min as described previously (20). We measured EGF-independent EGFR autophosphorylation after adding W-13 to serum-starved cells (see legend to Fig. 8), preparing the cell lysate as described previously (26).

Electrophoresis and Western Blot Analysis—Slab gel linear gradient (5–20% (w/v) polyacrylamide and 0.1% (w/v) SDS at pH 8.3) electrophoresis was performed according to Laemmli (45) at 12 mA overnight. Alternatively, we used 8% (w/v) polyacrylamide gels. Proteins were electrotransferred from the gel to a polyvinylidene difluoride/Immobilon-P membrane for 2–3 h at 300 mA in a medium containing 48 mM Tris-base, 36.6 mM L-glycine, 0.04% (w/v) SDS, and 20% (v/v) methanol; fixed with 0.2% glutaraldehyde in 25 mM Tris-HCl (pH 8), 150 mM NaCl, and 2.7 mM KCl (TNK buffer) for 45 min; and transiently stained with Fast Green FCF to ascertain the regularity of the transfer procedure. The PDF membrane was blocked with 5% (w/v) bovine serum albumin in 0.1% (w/v) Tween 20, 100 mM Tris-HCl (pH 8.8), 500 mM NaCl, and 0.25 mM KCl at pH 8.8 (T-TBS medium) and probed overnight with a 1:5000 dilution of the anti-phosphotyrosine antibody conjugated to horseradish peroxidase (RC20). The phosphotyrosine-containing 170-kDa EGFR band and 205-kDa EGFR-GFP bands were visualized following development with ECL reagents according to the manufacturer's instructions and exposure of x-ray films for appropriate periods of time.

When required, the intensity of the phosphorylated EGFR band was quantified with a computer-assisted scanning densitometer using the NIH Image 1.60 program. Corrections were made for small changes in the amount of protein present in the electrophoretic tracks as detected by Fast Green FCF staining followed by densitometric reading. To avoid any exposure time differences between gels loaded with samples corresponding to experiments performed in parallel, we exposed a single film to the different polyvinylidene difluoride membranes. Protein concentration was determined by the method of Lowry (46) using bovine serum albumin as a standard.

RESULTS

W-7/W-13/W-12 Bind Strongly to Phospholipid Membranes, Reducing the Magnitude of the Negative Zeta Potential—Fig. 1 shows how the acidic lipid PS produces a negative electrostatic potential in the aqueous phase adjacent to a phospholipid bilayer. The zeta potential, ζ, is the electrostatic potential close (~2 Å) to the surface of the membrane, as shown in Fig. 1*B*; ζ = −45 mV (*left points* in Fig. 3*A*) for the 2:1 PC/PS vesicles used for these measurements. Fig. 3*A* shows the effect of exposing the vesicles to W-7, W-13, or W-12. Adding 10–100 μM W-7/W-13 (the concentration range typically used in cell biology experiments) markedly reduces the magnitude of the zeta potential. For example, 10 or 30 μM W-7/W-13 reduces ζ by ~15 or ~20 mV, respectively. W-12, which is about 10-fold less potent as a CaM inhibitor (47, 48), decreases the magnitude of the zeta potential about 10-fold less effectively.

Fig. 3*B* illustrates the principle of the measurements; the schematic diagram shows an MLV moving in an electric field, with the *length* of the *arrow* indicating the velocity. We calculate ζ from the measured velocity/field, μ, using Equation 3. Fig. 3*C* shows that positively charged amphipathic weak bases, such as W-7, bind to the membrane surface and reduce its net negative charge. This decreases the magnitude of ζ, slowing the vesicle's velocity measured in a unit field; Equation 1 and the simple capacitor model of a diffuse double layer shown in Fig. 1*C* illustrate this effect. For example, adding 30 μM W-7/W-13 decreases the mobility/zeta potential ~50% (Fig. 3*A*); this implies a 50% reduction in the charge density on the surface of the vesicle or half as many positively charged W-7 adsorbed to the membrane as negatively charged PS in the outer leaflet. We note in passing that the velocity of the MLVs in an electric field is independent of their radius and depends only on the charge density on the outer leaflet, so only the inhibitors bound to this leaflet are illustrated in Fig. 3*C*. The neutral form of the weak base, *B*, crosses the membrane rapidly and recombines with a proton to form HB^+, which also binds to the inner leaflet of the MLV, or the inner leaflet of the plasma membrane in a cell.

TFP and CDZ Also Bind to Phospholipid Membranes—TFP binds to 2:1 PC/PS vesicles with ~3-fold higher affinity than W-7/W-13, as shown by comparing Figs. 4 and 3 (*e.g.* adding 30 μM TFP or 100 μM W-7/W-13 produces a similar effect on ζ). Note that TFP, like W-7 (data not shown), binds with equal affinity to 2:1 PC/PS and PC/PG vesicles (*black* and *white diamonds* in Fig. 4). This suggests that the acidic lipids PS and PG enhance the binding of TFP/W-7 to membranes through nonspecific electrostatic effects rather than through specific chemical interactions. Electrophoretic mobility experiments allow us to determine the relative importance of the electrostatic and hydrophobic components of the binding. We measured the binding of TFP to electrically neutral PC vesicles, which do not move in an electric field (*i.e.* ζ = 0 mV) (Fig. 4, *gray diamond* on the *left*); exposing the PC vesicles to TFP produces a positive zeta potential (*gray diamonds* in Fig. 4). Gouy-Chapman-Stern theory (32) can describe quantitatively the hydrophobic binding of amphipathic weak acids or bases to PC vesicles (see Fig. 6 in Ref. 49) and their effect on the zeta potential. The only adjustable parameter is the molar partition coefficient, *K*, of TFP onto the surface of PC membranes (K = 10^4 M^{-1}; see Ref. 50 for a detailed theoretical description of TFP binding to PC). This is *equivalent* to assuming $K_d = 10^{-4}$ M for TFP binding to an individual lipid or that TFP partitions hydrophobically with an energy of ~6 kcal/mol onto the surface. Earlier work (50) showed an apparent $K_d = 10^{-5}$ M, describing the effect of TFP on the zeta potential of the membranes containing 30% acidic

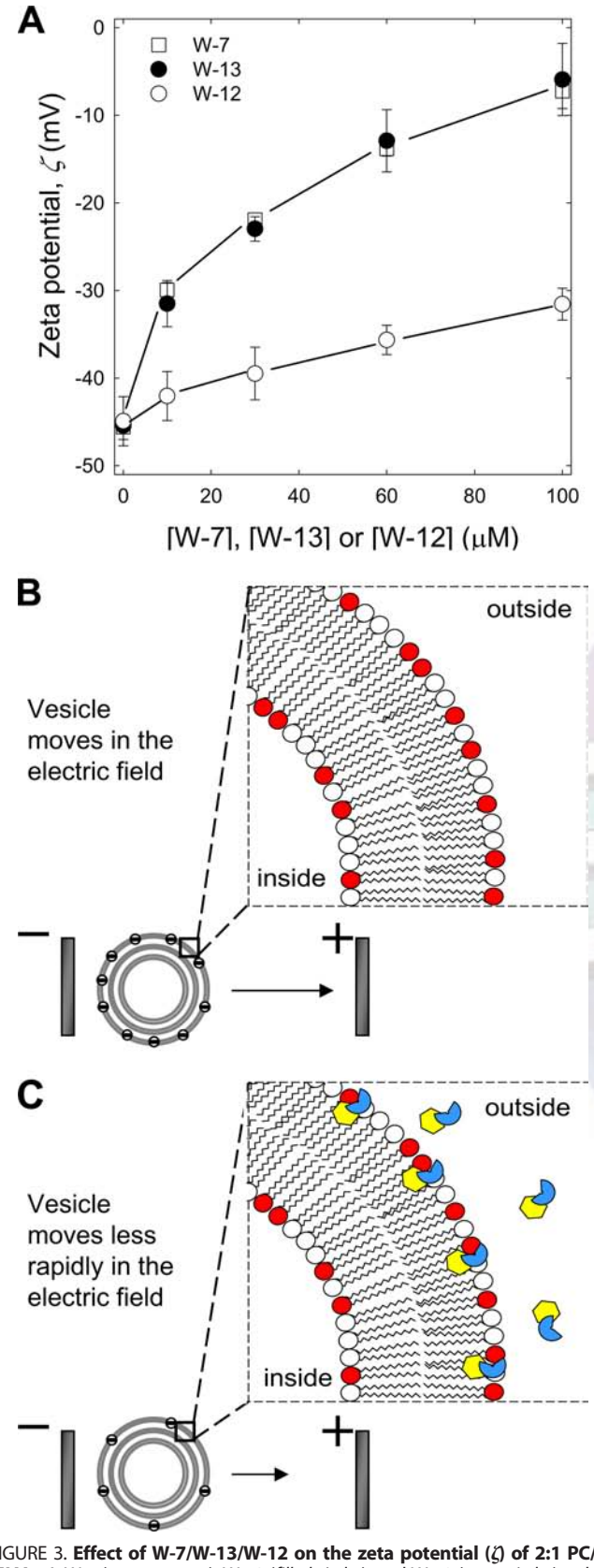

FIGURE 3. **Effect of W-7/W-13/W-12 on the zeta potential (ζ) of 2:1 PC/PS MLVs.** *A*, W-7 (*open squares*), W-13 (*filled circles*), and W-12 (*open circles*) reduce the zeta potential of phospholipid vesicles. The aqueous solutions contain 100 mM KCl, 1 mM MOPS, pH 7.0. Each point on the graph represents >20 measurements ± S.D., when larger than the size of the *symbol*. Note that exposing the vesicles to 10 μM W-7 or W-13 produces a significant change in ζ, from −45 to −30 mV. W-12, which lacks the hydrophobic chloro group of W-7/W-13 (Fig. 2), binds to the bilayer and reduces its charge density, and consequently the magnitude of ζ, about 10-fold less effectively. *B*, schematic diagram of a multilamellar vesicle moving in an electric field (indicated with *plus* and *minus* electrodes) with a velocity proportional to the *length* of the *arrow*. The *inset* shows an expanded region of the lipid bilayer with negative PS lipids (*red*). *C*, schematic diagram of a multilamellar vesicle in the presence of calmodulin inhibitors (these positive/hydrophobic molecules are represented in *blue*/*yellow* in the *inset*). The calmodulin inhibitors shown in Fig. 2 are amphipathic weak bases. The positively charged inhibitors bind to a membrane containing acidic lipids (*red*) and reduce its surface charge density (σ); this reduces the velocity (μ) of the vesicle in the electric field (indicated by a *shorter arrow* in the schematic diagram) and the zeta potential (ζ). See Equations 1 and 3 and "Experimental Procedures."

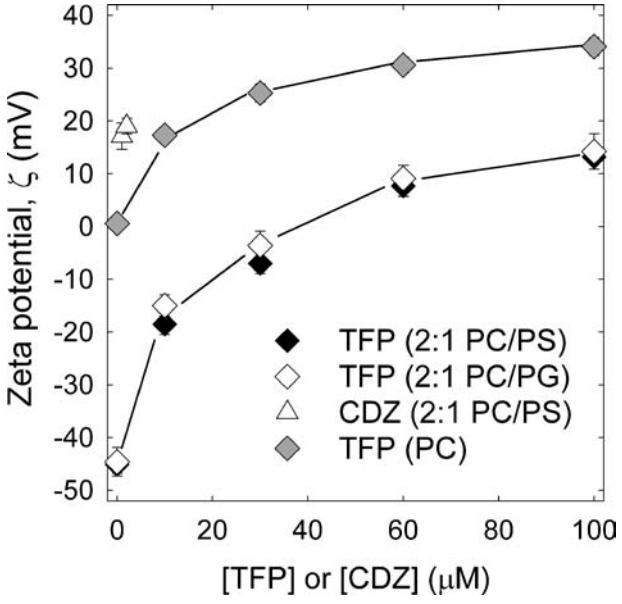

FIGURE 4. **Effect of TFP and CDZ on the zeta potentials of phospholipid vesicles.** TFP binds equally well to 2:1 PC/PS (*black diamonds*) and 2:1 PC/PG (*white diamonds*) vesicles through a combination of nonspecific hydrophobic and electrostatic interactions. It binds to PC vesicles (*gray diamonds*) through hydrophobic interactions only. CDZ binds strongly to the 2:1 PC/PS vesicles (*white triangles*); 1 μM CDZ reverses the charge on 2:1 PC/PS vesicles and produces a positive zeta potential ($\zeta = +17$ mV).

lipid; the 10-fold increase in affinity for these negatively charged membranes is due to the Boltzmann effect illustrated in Fig. 1. In other words, nonspecific electrostatics concentrates the monovalent cationic TFP by ~10-fold adjacent to the surface of the PC/PS membrane, where they then adsorb hydrophobically. Thus, the overall binding energy to 2:1 PC/PS vesicles, 7.5 kcal/mol, comprises contributions from both nonspecific electrostatic (1.5 kcal/mol) and hydrophobic (6 kcal/mol) interactions. Importantly, TFP binds to 2:1 PC/PS membranes and Ca^{2+}/CaM with about the same affinity: K_d of ~10 μM (Fig. 4) and ~5 μM (51, 52), respectively.

CDZ binds to membranes with such high affinity that technical limitations preclude accurate zeta potential measurements for [CDZ] < 1 μM. Adding 1 μM CDZ reverses the charge on a 2:1 PC/PS vesicle, changing ζ from −45 to +17 ± 2 ($n = 8$) mV; 2 μM CDZ changes the zeta potential to +19 ± 1.5 ($n = 16$) mV, as shown in Fig. 4 (*triangles*). Note that 1 μM CDZ exerts a larger effect on the zeta potential of 2:1 PC/PS vesicles than 100 μM TFP (Fig. 4). Application of the Gouy-Chapman-Stern theory (32, 49) to these data shows that the affinity of CDZ for these membranes is >100-fold stronger than that of W-7/

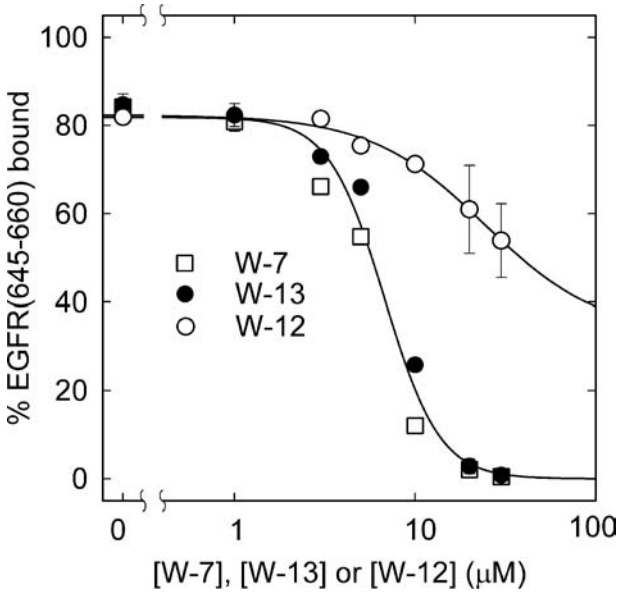

FIGURE 5. **Effect of calmodulin inhibitors on the membrane binding of EGFR-(645–660), a peptide corresponding to the basic juxtamembrane region of the intrinsic membrane protein.** Binding of radioactively labeled EGFR-(645–660) peptide to 20 μM 2:1 PC/PS LUVs in the presence of different concentrations of W-7 (*open squares*), W-13 (*filled circles*), and W-12 (*open circles*) was measured using a centrifugation technique. The solutions contained 100 mM KCl, 10 mM MOPS at pH 7. Each point on the graph is an average of more than four measurements ± S.D., when larger than the size of the *symbol*.

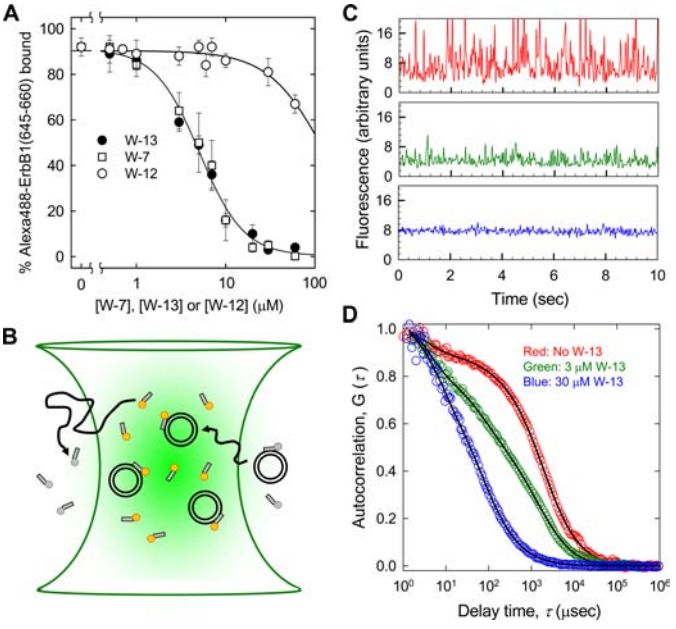

FIGURE 6. **FCS measurements of the effect of calmodulin inhibitors on the membrane binding of EGFR-(645–660).** *A*, binding of Alexa 488-labeled EGFR-(645–660) to 20 μM 1:1 PC/PS LUVs in presence of different concentrations of W-7 (*open squares*), W-13 (*filled circles*), and W-12 (*open circles*) measured using FCS. The peptide concentration is 2–4 nM in solutions containing 100 mM KCl, 1 mM MOPS buffer at pH 7. Each point on the graph is an average of more than six measurements ± S.D., when larger than the size of the *symbol*. Note that exposure of the vesicles to 10 μM W-7 or W-13 reduces EGFR-(645–660) binding from 90 to 15%. W-12 reduces binding about 10-fold less effectively. *B*, schematic diagram of the optically defined confocal open volume (*green*) of an FCS instrument. Fluorescent molecules (in our experiment, peptides with an Alexa 488 label (*gray rods* with *orange circles*) that are free or bound to LUVs (*black donuts*)) diffuse through this volume, producing temporal fluctuations in the fluorescence signal. *C*, fluorescence signal (*time traces*) obtained from three different solutions containing 4 nM Alexa 488-EGFR-(645–660), 20 μM 1:1 PC/PS LUVs in different concentrations of W-13: 0 μM (*red*), 3 μM (*green*), and 30 μM (*blue*). The temporal autocorrelation function, $G(\tau)$ is calculated from each of these time traces. *D*, normalized temporal autocorrelation functions, $G(\tau)$, calculated from data presented in *C* and using the same *color code*. Fitting the autocorrelation functions (*black lines*) to a two-component diffusion equation (Equation 6) produces the percentage of peptide bound to LUVs; 92% peptide is bound in 0 μM W-13 (*red*), 60% in 3 μM W-13 (*green*), and 2% in 30 μM W-13 (*blue*). The data in *A* combine the results of similar measurements and analysis for different concentrations of W-7, W-13, and W-12.

W-13/TFP, an observation that is qualitatively consistent with the former's ~1000-fold higher affinity for Ca^{2+}/CaM (51).

Calmodulin Inhibitors Also Reduce Binding of Basic Peptides to Membranes—If 30 μM W-7 decreases the magnitude of the potential at the surface of the plasma membrane by ~20 mV, as it does for 2:1 PC/PS membranes (Fig. 3*A*), the Boltzmann relation predicts that it should greatly decrease the electrostatic binding of basic clusters on numerous peripheral and intrinsic membrane proteins (*e.g.* Src, K-Ras4B, MARCKS, gravin, and the cytoplasmic JM region of the EGFR, respectively). We illustrate this effect by measuring the effect of W-7 on the binding of EGFR-(645–660), a +8 valent basic/hydrophobic peptide (sequence RRRHIVRKRTLRRLLQ) to 2:1 PC/PS membranes. This peptide corresponds to the putative Ca^{2+}/CaM and membrane-binding JM region of the EGFR.

We first analyze the expected result qualitatively, assuming (incorrectly) that EGFR-(645–660) is a point charge of valence $z = +8$ that does not perturb the potential. The Boltzmann relation predicts that the $\Delta\psi = 20$ mV decrease in the magnitude of the surface potential by 30 μM W-7/W-13 should decrease in the local concentration of the peptide at the membrane solution interface >100-fold ($\exp(-ze\Delta\psi/kT) = 10^{z\Delta\psi/60}$) and thus decrease the binding >100-fold. Measurements of peptide binding *versus* lipid concentration do indeed show that 30 μM W-7/W-13 decreases the molar partition coefficient (reciprocal of the lipid concentration required to bind 50% of the peptide) of EGFR-(645–660) 100-fold, from 10^6 to 10^4 M^{-1} (data not shown).

F5 Fig. 5 shows how the membrane binding of EGFR-(645–660) depends on the concentration of W-7/W-13/W-12 for a lipid concentration that initially binds most of the peptide. Note that 10 μM W-7/W-13 decreases the binding markedly; only ~20% of the peptide remains bound to the vesicles. (As expected, 10 μM W-7 exerted a similarly large effect on the membrane binding of a different basic/hydrophobic peptide corresponding to the effector domain of MARCKS; data not shown.) W-12 decreases the binding of the peptide ~10-fold less effectively than W-7/W-13, consistent with its smaller effect on the zeta potential (Fig. 3*A*). We confirmed the results of experiments shown in Fig. 5, which used a centrifugation technique to separate free radioactively labeled peptide from that bound to LUVs, by performing FCS experiments with a fluorescently labeled peptide; the results, shown in Fig. 6, are essentially the same. AQ: Q F6

Fig. 6*A* shows how W-7/W-13/W-12 affect membrane binding of Alexa 488 EGFR-(645–660); 10 μM W-7 or W-13 decreases the binding markedly, from ~90 to ~15%; W-12 is ~10-fold less effective. Fig. 6*B* illustrates the principle of these FCS binding measurements; Rusu *et al.* (35) discuss the bio-

physical aspects of these measurements in more detail. The schematic diagram depicts peptides as *gray rectangles* with *orange circles* and LUVs as *black donuts*. The free peptides diffuse through the optically defined observation volume (*green*, diameter ~0.3 μm) of the FCS instrument more rapidly than peptides bound to the relatively large LUVs. This diffusion produces temporal fluctuations in the fluorescence signal, evident in the time traces (Fig. 6*C*). The temporal autocorrelation functions, $G(\tau)$ values (Fig. 6*D*), are calculated from these time traces. Fitting the autocorrelation functions to a two-component diffusion equation (Equation 6) yields the percentage of peptide bound to the LUVs. The experiments show that W-13 alters EGFR-(645–660) binding to LUVs; 92% peptide is bound in 0 μM W-13 (*red*), 60% peptide is bound in 3 μM W-13 (*green*), and 2% peptide is bound in 30 μM W-13 (*blue*). Fig. 6*A* summarizes the FCS results from experiments performed with different concentrations of W-7, W-13, and W-12.

Summary of Results Obtained with Model Membranes and Predictions about Inhibitor Effects on Cells—The membrane-permeable CaM inhibitors illustrated in Fig. 2, which all bind to membranes through hydrophobic/electrostatic interactions at about the same concentrations that they bind to Ca^{2+}/CaM, are used widely in cell biology. Extrapolating the results on model membranes to the inner leaflet of the plasma membrane suggests that these inhibitors will reduce the magnitude of the negative electrostatic surface potential (Figs. 3 and 4) and decrease the electrostatic binding of clusters of positively charged residues to the membrane (Figs. 5 and 6). Although one must obviously be cautious when interpreting cell biological experiments with CaM inhibitors, we do wish to suggest that they can provide useful information about cellular processes. For example, Ca^{2+}/CaM binds to the EGFR (18, 20) and to peptides corresponding to its JM region (19, 21, 53). Does this binding contribute to the activation of the receptor? EGF-mediated dimerization of EGFR (11) produces a transient increase in the level of free $[Ca^{2+}]_i$ (12–17), and thus Ca^{2+}/CaM; our *working hypothesis* is that this transient elevation in Ca^{2+}/CaM contributes to the observed transient pulse of EGFR autophosphorylation observed in many different cell types (20, 54, 55). The observation that calmodulin inhibitors suppress the initial transient pulse of EGFR autophosphorylation in several cell types is consistent with the hypothesis (20, 21).

To further test our hypothesis, we exposed cells to a calcium ionophore before adding EGF; the ionophore should increase the steady-state level of $[Ca^{2+}]_i$ and thus Ca^{2+}/CaM. The hypothesis makes two obvious predictions about the effect of this treatment: (i) adding EGF should produce a consistently high level of EGFR autophosphorylation, and (ii) W-13 should decrease autophosphorylation at all times after the addition of EGF.

Effect of W-13 on EGF-dependent Autophosphorylation of EGFR—The increase in $[Ca^{2+}]_i$ that results from exposing a cell to the Ca^{2+} ionophore A23187 will have many effects. For example, it will activate both protein kinase C and calcium/calmodulin-activated kinase II, both of which inhibit EGFR autophosphorylation (56–62); thus, we added inhibitors of these EGFR regulatory protein kinases before exposing cells to the Ca^{2+} ionophore. Fig. 7*A* illustrates the results from a control experiment in N7 × HERc cells treated with KN-93 and GF109203X, inhibitors of calcium/calmodulin-activated kinase II and protein kinase C, respectively. In the absence of W-13 (*open symbols*), adding EGF produces rapid EGFR autophosphorylation that reaches a maximum after ~2 min and then declines to a plateau after ~15 min. In the presence of W-13 (*filled symbols*), the initial pulse is absent, but the steady state value is unchanged, as expected from our hypothesis. These results reflect closely earlier studies on cells not treated with calcium/calmodulin-activated kinase II and protein kinase C inhibitors (see Fig. 4*A* of Ref. 20). The simplest interpretation of Fig. 7*A* is that W-13 inhibits Ca^{2+}/CaM, which is needed to produce the transient maximum in EGF-mediated EGFR autophosphorylation.

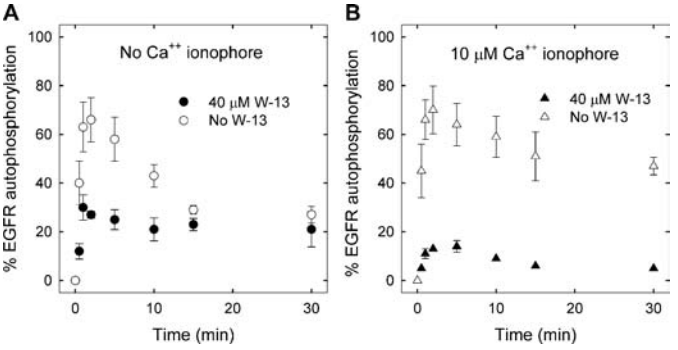

FIGURE 7. **Effect of W-13 (*filled symbols*) on EGF-dependent EGFR autophosphorylation in the absence (*A*) or presence (*B*) of a calcium ionophore, A23187.** *A*, serum-starved N7 × HERc cells were incubated for 1 h at 37 °C with 10 μM KN-93 (calcium/calmodulin-activated kinase II inhibitor), and then 10 μM GF109203X (protein kinase C inhibitor) was added, and the cells were maintained for an additional 1 h. Thereafter, the cells were incubated in the absence (*open symbols*) and presence (*filled symbols*) of 15 μg/ml (40 μM) W-13 for 30 min at room temperature (22 °C), followed by the addition of 10 nM EGF. The reaction was arrested with ice-cold 10% (w/v) trichloroacetic acid at the indicated times after EGF addition. *B*, serum-starved N7 × HERc cells were treated with 10 μM KN-93 plus 10 μM GF109203X as above and then incubated in the absence (*open symbols*) and presence (*filled symbols*) of 15 μg/ml (40 μM) W-13 for 15 min at room temperature (21–23 °C). We added 5 μg/ml (9.5 μM) A23187 (calcium ionophore) and incubated the cells for an additional 15 min before adding 10 nM EGF. The reaction was arrested at the indicated times after the addition of EGF as above. Samples in *A* and *B* were processed for SDS-PAGE and Western blot using an anti-phosphotyrosine antibody (RC20); densitometry of the 170-kDa phosphorylated EGFR band was performed as indicated under "Experimental Procedures." The *ordinates* represent the mean ± S.D. of three (*A*) or two (*B*) independent experiments, relative to control experiments (100%) performed in the absence of both inhibitors and ionophore. Control cells were treated with 10 nM EGF for 1 min. *Error bars* are shown if larger than the *symbol*.

Fig. 7*B* shows results from experiments in cells treated with A23187 (plus the two kinase inhibitors) prior to the addition of EGF, which agree with the two predictions of our working hypothesis. First, the plateau or steady state level of EGFR autophosphorylation is higher (compare *open symbols* in Fig. 7, *A* and *B*). Second, adding W-13 reduces not only the initial phase of EGFR autophosphorylation but also the level observed after longer times (Fig. 7, compare *A* and *B*). This important result supports our hypothesis that Ca^{2+}/CaM enhances EGFR autophosphorylation mediated by EGF, at least in this cell type. (We report additional control experiments with a peptide inhibitor of Ca^{2+}/CaM and experiments designed to test the hypothesis that Ca^{2+}/CaM acts directly on the EGFR in the supplemental materials.)

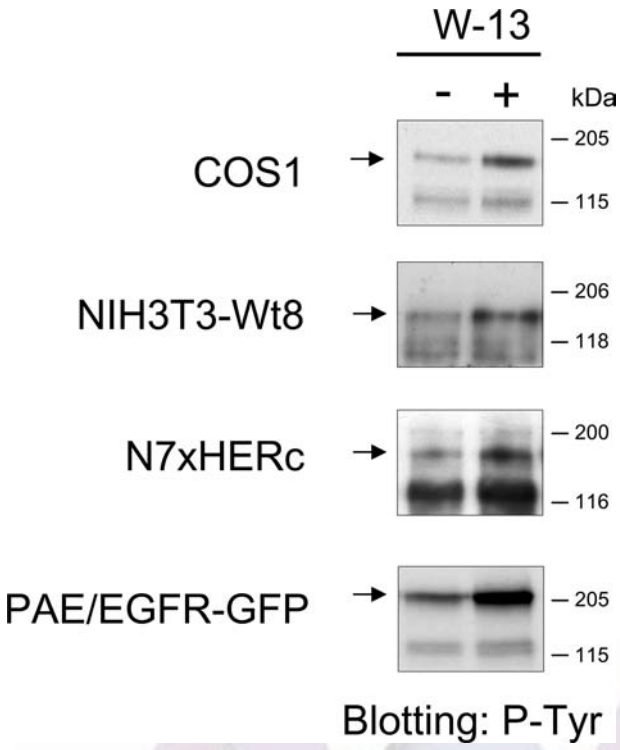

FIGURE 8. **W-13 increases tyrosine phosphorylation of EGFR in different cell lines.** Four different cell lines were serum-starved overnight and then incubated with 10 μg/ml (29 μM) W-13 for 10 min at 37 °C. Lysates normalized to an equal amount of protein were subjected to electrophoresis and then analyzed by Western blot with an antiphosphotyrosine (*P-Tyr*) antibody (RC20); the *arrow* indicates phosphorylated EGFR.

W-13 Stimulates EGFR Phosphorylation in the Absence of EGF—We previously reported W-13 and W-7 *stimulate* EGFR activation in COS-1 cells in the *absence* of EGF or other ligand (21, 27); we investigated whether this effect is more general by measuring EGFR tyrosine autophosphorylation after W-13 treatment in four different cell lines. Cultures of NIH3T3 (wt8), COS-1, and N7 × HERc cells expressing human EGFR or porcine aortic endothelial cells expressing a chimeric EGFR with GFP at its C terminus (PAE/EGFR-GFP) were starved overnight, treated with 10 μg/ml (~30 μM) W-13 for 10 min, and prepared as cell lysates for Western blot analysis with a monoclonal anti-phosphotyrosine antibody. W-13 treatment increased EGFR-phosphotyrosine levels in each cell type (Fig. 8). (The band at 170 kDa corresponds to the EGFR, and the band at 205 kDa corresponds to the chimeric receptor. PAE cells do not express detectable levels of endogenous EGFR). As discussed in more detail below, one explanation for these effects is that W-13 binds to the inner leaflet of the plasma membrane, reducing the magnitude of the negative electrostatic surface potential (*e.g.* Fig. 3), allowing the positively charged JM region (residues 645–660) of the EGFR to desorb from the membrane more easily (see Figs. 4 and 5) and thus mimicking the action of Ca^{2+}/CaM in EGF-stimulated cells.

DISCUSSION

Our most important results, shown in Fig. 7, support the hypothesis that Ca^{2+}/CaM plays a role, albeit probably a minor one, in the EGF-mediated activation of the EGFR. Our experiments on model membranes (Figs. 3 and 4) also indicate that the commonly used membrane-permeable Ca^{2+}/CaM inhibitors shown in Fig. 2 should all bind significantly to the inner leaflet of the plasma membrane at approximately the same concentrations at which they are used to inhibit calmodulin in cells. Thus, the common assumption that using two chemically different inhibitors (*e.g.* TFP and W-7) provides evidence that they are acting on specifically on calmodulin is not correct. The inhibitors bind to and have concomitant effects on the plasma membrane that complicate interpretation of the cellular effects. The inhibitors shown in Fig. 2 bind to membranes and to the hydrophobic pocket of Ca^{2+}/CaM (63, 64) via nonspecific hydrophobic and electrostatic interactions (Figs. 3 and 4). Because the membrane-binding results in Figs. 3–6 may be of general interest to cell biologists, we discuss them before the EGFR results.

Membrane Binding Allows the Molecules Shown in Fig. 2 to Function Efficiently as Ca^{2+}/CaM Inhibitors in Living Cells—The membrane binding of the Ca^{2+}/CaM inhibitors documented in Figs. 3 and 4 is not without a fortuitous side effect. We argue, in the supplemental materials, that they would not be useful Ca^{2+}/CaM inhibitors in a cell if they did not bind strongly to membranes. Specifically, we argue that the plasma and intracellular membranes act as reservoirs of the calmodulin inhibitors, binding most of the inhibitor that enters the quiescent cell and rapidly releasing the inhibitor to bind Ca^{2+}/CaM when the level of $[Ca^{2+}]_i$ rises in the cell.

Effects of Calmodulin Inhibitors Binding to the Inner Leaflet of the Plasma Membrane—Our observations suggest that cellular studies using high concentrations of weak base Ca^{2+}/CaM inhibitors can be complicated by a wide variety of membrane binding effects. We discuss three side effects; more are likely. (i) Many important peripheral proteins, such as Src, KRas4B, gravin, AKAP79, MARCKS, and HIVgag, require electrostatic interactions to adhere to the plasma membrane (7, 8, 65–67). These proteins all contain one or more clusters of basic residues that interact with the negative electrostatic surface potential produced by acidic lipids in the plasma membrane (Fig. 1). High inhibitor concentrations weaken these interactions, and, if the net negative charge on the inner leaflet becomes sufficiently low, these proteins will desorb from the membrane and translocate to the cytoplasm. Clusters of basic residues on intrinsic membrane proteins, such as the EGFR, should also bind less strongly to membranes when the Ca^{2+}/CaM inhibitors are present. Figs. 5 and 6 show that the inhibitors produce the expected desorption of a basic peptide from a model phospholipid membrane. We suspect that the action of these calmodulin inhibitors on membranes could be responsible for a significant fraction of their many observed effects on cells. To cite just one example of a peripheral protein, Young *et al.* (68) showed that 50 μM W-7 prevents the binding of sphingosine kinase to the plasma membrane and reasonably attributed this effect to W-7 inhibiting Ca^{2+}/CaM; recent mutation experiments appear to support this interpretation (69). Our results, however, suggest that this effect could equally well be due to W-7 reducing the surface potential of the plasma membrane, particularly because acidic lipids appear to mediate the membrane association of sphingosine kinase (70). An example of an inte-

gral membrane protein is the polymeric immunoglobulin receptor, pIgR, which has a 17-residue membrane-proximal cytoplasmic segment, residues 653–670, that binds Ca^{2+}/CaM with high affinity (71). In the absence of Ca^{2+}/CaM, this segment probably also binds to the negatively charged inner leaflet of the plasma membrane, since it has a net charge of +5. Experiments show that 15–150 μM W-13, W-7, and TFP all inhibit transcytosis of the pIgR (72); these concentrations also reduce the net charge density of a membrane significantly (Figs. 3 and 4). Thus, the available data do not distinguish whether transcytosis inhibition is due to Ca^{2+}/CaM inhibition or plasma membrane effects or both. (ii) The positively charged HB^+ form of the weak base inhibitors will bind more strongly to the inner than to the outer leaflet of the plasma membrane, because the inner leaflet contains 100% of the major acidic lipid PS and is thus more negatively charged. The resulting differential increase in lateral surface pressure on the inner leaflet will induce a "bilayer couple" effect that may cause curvature of the plasma membrane, as discussed in the classic paper by Sheetz and Singer (73) and in subsequent reports (74). They exposed erythrocytes to amphipathic weak bases, such as local anesthetics, chlorpromazine, etc., to induce the bilayer couple effect; the amphipathic weak bases in Fig. 2 should produce similar effects. (iii) Because the positively charged HB^+ form of the weak base binds more strongly to the inner than to the outer leaflet of the plasma membrane, the magnitude of the transmembrane electric field within the membrane will decrease. Voltage-gated ion channels have voltage sensors located within the membrane that will sense this change and respond to it as to a depolarization, even in the absence of a change in the measurable potential difference between the bulk aqueous solutions outside and inside the cell (75). This could open ion channels permeable to Ca^{2+}, increasing $[Ca^{2+}]_i$. High concentrations (>100 μM) of W-7 are known to increase $[Ca^{2+}]_i$ (76, 77), but these concentrations are well above the level required to inhibit Ca^{2+}/CaM.

The inhibitors shown in Fig. 2 could produce these and numerous other effects due to binding to membranes in living cells; nevertheless, we argue below that they remain useful tools for studying the role of calmodulin in cellular processes.

Using Inhibitors to Investigate the Role of Calmodulin in the EGF-mediated Activation of the EGFR—The activation and trafficking of the EGFR have been reviewed elsewhere (78–81). Villalobo and co-workers (18, 20) showed that EGFR is a Ca^{2+}/CaM-binding protein. What is the physiological significance of this binding in EGF-mediated activation of EGFR? The question is important, because the EGFR activation mechanism differs from that of most other receptor tyrosine kinases. Specifically, the activation loop in the EGFR kinase domain is not phosphorylated when the receptor binds its ligand and undergoes dimerization (79). A recent report from the Kuriyan laboratory provides strong evidence that when EGF mediates EGFR dimer formation, the kinase domain of one EGFR in the dimer pair binds to and activates the other, changing the conformation of its activation loop by an allosteric mechanism (22, 23). But other autoinhibitory mechanisms may exist for the EGFR family, as they do for other receptor tyrosine kinases (82). Factors that remove these extra autoinhibitory mechanisms may act in parallel with the allosteric activation mechanism described by Zhang *et al.* (22). For example, Landau *et al.* (83) proposed that a portion of the C-terminal domain binds directly to and inhibits the kinase domain; McLaughlin *et al.* (21) hypothesized that the positively charged residue 645–660 region of the JM domain and the positive face of the kinase domain bind electrostatically to the plasma membrane, contributing to autoinhibition.

Our working hypothesis in this report is that Ca^{2+}/CaM releases an autoinhibitory function, probably by binding to the EGFR JM region. Stimulation by EGF produces only a transient increase in $[Ca^{2+}]_i$, suggesting that Ca^{2+}/CaM should contribute to the initial pulse of EGFR autophosphorylation but not to the steady state level. Other groups have proposed alternative explanations for the initial transient peak in autophosphorylation; *e.g.* Kholodenko *et al.* (54, 55) suggested that the peak is due to binding of Src homology 2-containing proteins/adaptors to the Tyr(P) residues, providing temporary protection from the action of phosphatases. We attempted to distinguish between our working hypothesis and other models that do not involve Ca^{2+}/CaM via experiments with the calmodulin inhibitor W-13. Li *et al.* (20) and others (21) showed that appropriate concentrations of W-7/W-13/W-12 do indeed inhibit the initial transient maximum, but not the steady state level, of EGF-mediated EGFR autophosphorylation in different cell types (*e.g.* N7 × HERc fibroblasts, COS1 monkey kidney cells). Fig. 7*A* shows similar effects in cells examined under different conditions (inhibitors for calcium/calmodulin-activated kinase II and protein kinase C present). Note that this inhibition is observed in many but not all cell types; W-7 did not affect EGF-mediated EGFR autophosphorylation kinetics in hepatocytes.[5] Furthermore, Li *et al.* (20) noted that with cells overexpressing EGFR, such as EGFR-T17 and A431, the calmodulin inhibitor W-13 was effective only if the cells were first exposed to a calcium ionophore.

Two obvious corollaries emerge from our hypothesis that Ca^{2+}/CaM is important for the initial phase of the EGFR autophosphorylation. First, maintaining high levels of Ca^{2+} and thus Ca^{2+}/CaM (*e.g.* by exposing the cell to a Ca^{2+} ionophore) should increase the steady state level of EGFR autophosphorylation after EGF-mediated dimerization. Second, under these conditions, a Ca^{2+}/CaM inhibitor, such as W-13, should reduce EGFR autophosphorylation at all times after the addition of EGF, not just during the initial phase. The data in Fig. 7*B* are consistent with these two predictions and support the hypothesis that Ca^{2+}/CaM augments EGFR autophosphorylation. This raises the question of where Ca^{2+}/CaM is acting: directly on the EGFR or indirectly through some other Ca^{2+}/CaM dependent process? We addressed this question by testing the effect of W-13 on cells expressing an EGFR mutant in which the only known Ca^{2+}/CaM binding region on the protein, residues 645–660 in the cytoplasmic JM region, is disrupted by insertion of an acidic 23-amino acid sequence; the inhibitor does not affect autophosphorylation of this mutant (Fig. S1*B*).

In summary, the simplest explanation of the results in Figs. 7 and S1 is that Ca^{2+}/CaM binds to the JM region and augments

[5] J. Hoek, personal communication.

the initial phase of the EGF-mediated EGFR autophosphorylation; the specific mechanism for this augmentation and its role in the more general allosteric mechanism for activation of the kinase domain described by Zhang *et al.* (22) remains to be determined. Two proposed models could account for these data; the basic JM region could bind to a cluster of acidic residues in the C-terminal tail region of an adjacent EGFR (84) or to acidic phospholipids in the membrane (21). Recent experiments support the claim that the JM region can bind with high affinity to the inner leaflet of the plasma membrane. Specifically, NMR and fluorescence measurements on peptides corresponding to transmembrane plus JM domains of EGFR reconstituted into phospholipid vesicles (25) show the transmembrane helix breaks at the membrane-solution interface, and the extended JM region binds to the membrane if it contains acidic lipids (either 1% inositol 1,4,5-bisphosphate or >5% PS); adding Ca^{2+}/CaM can release the JM region from the membrane.

Evidence That Calmodulin Inhibitors Can Activate EGFR in the Absence of Ligand by Binding to Membranes—In the *absence* of EGF, adding W-13 to four different cell types *activates* EGFR (Fig. 8). The simplest interpretation of this result is that W-13 can activate EGFR autophosphorylation through an effect *other* than binding to Ca^{2+}/CaM, possibly through binding to the inner leaflet of the plasma membrane. There are many ways this activation might occur. In the electrostatic engine model (21), for example, either reducing the electrostatic attraction of the JM + kinase domains for the plasma membrane or binding of Ca^{2+}/CaM to the JM region should release autoinhibition, as illustrated in Refs. 7, 21, and 25. Figs. 5 and 6 in this report show that W-13 releases a simple peptide corresponding to the EGFR JM region from a phospholipid vesicle.

This model predicts that other weak bases that do *not* act as CaM inhibitors should also activate EGFR at the same concentration at which they bind to membranes. For example, the hydrophobic tail of sphingosine is tall and skinny in contrast to the short and broad hydrophobic regions of the inhibitors shown in Fig. 2; one expects micromolar concentrations of sphingosine to bind more strongly to membranes than to the hydrophobic pocket of Ca^{2+}/CaM, and experiments confirm this expectation (data not shown). As expected from the model, sphingosine activates EGFR in the absence of EGF (85) at the same concentration (2 μM) at which it binds to membranes and reverses the sign of the zeta potential (21). Furthermore, fluorescence experiments show that sphingosine causes the JM region of reconstituted transmembrane + JM EGFR peptides to desorb from bilayer membranes (25).

Conclusions—A model proposing that membrane binding of the JM and kinase domains contributes to autoinhibition of EGFR (21) predicts both of our key observations of the action of W-13 on the EGFR: its ability to inhibit EGF-mediated autophosphorylation (Fig. 7) *and* its ability to stimulate autophosphorylation of EGFR in the absence of EGF (Fig. 8). These dual effects are difficult to explain with other models for autoinhibition (*e.g.* see Landau *et al.* (83)). Specifically, one simple interpretation of our EGFR results is that calmodulin inhibitors decrease the EGF-mediated autophosphosphorylation by preventing Ca^{2+}/CaM from removing the positively charged EGFR JM region from the negatively charged plasma membrane (see Fig. 6 of Ref. 7); slightly higher concentrations of inhibitors stimulate the autophosphorylation in the absence of EGF by decreasing the net negative charge on the membrane, which facilitates desorption of the JM + kinase region from the membrane. In both cases, activation of the kinase domain and subsequent autophosphorylation of the EGFR in its C-terminal tail region presumably requires juxtaposition of the kinase domains and repositioning of the activation loop by the allosteric mechanism described by Kuriyan and co-workers (22). Thus, the JM region of the EGFR may play its autoinhibitory role by binding to the membrane and decreasing the collision frequency of the two kinase domains in an EGFR dimer. As reviewed elsewhere (82), the JM regions of many different receptor tyrosine kinases provide an additional secondary layer of autoinhibition, which complements the primary role played by the activation loop in the kinase domain.

Acknowledgments—We thank Andrey Sorokin (Medical College of Wisconsin, Milwaukee, WI), Alexander Sorkin (School of Medicine, University of Colorado), and Axel Ullrich (Max-Planck-Institut für Biochemie, Martinsried, Germany) for donating cell lines, Jan B. Hoek (Thomas Jefferson University, Philadelphia, PA) for valuable discussions, and William Woturski (Department of Physiology, HSC, State University of New York at Stony Brook) for excellent technical assistance.

REFERENCES

1. Clapham, D. E. (1995) *Cell* **80,** 259–268
2. Berridge, M. J., Bootman, M. D., and Roderick, H. L. (2003) *Nat. Rev. Mol. Cell Biol.* **4,** 517–529
3. Chin, D., and Means, A. R. (2000) *Trends Cell Biol.* **10,** 322–328
4. Hoeflich, K. P., and Ikura, M. (2002) *Cell* **108,** 739–742
5. Vetter, S. W., and Leclerc, E. (2003) *Eur. J. Biochem.* **270,** 404–414
6. Yamniuk, A. P., and Vogel, H. J. (2004) *Mol. Biotechnol.* **27,** 33–57
7. McLaughlin, S., and Murray, D. (2005) *Nature* **438,** 605–611
8. Yeung, T., Terebiznik, M., Yu, L., Silvius, J., Abidi, W. M., Philips, M., Levine, T., Kapus, A., and Grinstein, S. (2006) *Science* **313,** 347–351
9. McLaughlin, S. (2006) *Science* **314,** 1402–1403
10. Heo, W. D., Inoue, T., Park, W. S., Kim, M. L., Park, B. O., Wandless, T. J., and Meyer, T. (2006) *Science* **314,** 1458–1461
11. Ferguson, K. M. (2004) *Biochem. Soc. Trans.* **32,** 742–745
12. Pandiella, A., Magni, M., Lovisolo, D., and Meldolesi, J. (1989) *J. Biol. Chem.* **264,** 12914–12921
13. Cheyette, T. E., and Gross, D. J. (1991) *Cell Regul.* **2,** 827–840
14. Hughes, A. R., Bird, G. S., Obie, J. F., Thastrup, O., and Putney, J. W., Jr. (1991) *Mol. Pharmacol.* **40,** 254–262
15. Bezzerides, V. J., Ramsey, I. S., Kotecha, S., Greka, A., and Clapham, D. E. (2004) *Nat. Cell Biol.* **6,** 709–720
16. Li, W. P., Tsiokas, L., Sansom, S. C., and Ma, R. (2004) *J. Biol. Chem.* **279,** 4570–4577
17. Uyemura, T., Takagi, H., Yanagida, T., and Sako, Y. (2005) *Biophys. J.* **88,** 3720–3730
18. Li, H., and Villalobo, A. (2002) *Biochem. J.* **362,** 499–505
19. Martin-Nieto, J., and Villalobo, A. (1998) *Biochemistry* **37,** 227–236
20. Li, H., Ruano, M. J., and Villalobo, A. (2004) *FEBS Lett.* **559,** 175–180
21. McLaughlin, S., Smith, S. O., Hayman, M. J., and Murray, D. (2005) *J. Gen. Physiol* **126,** 41–53
22. Zhang, X., Gureasko, J., Shen, K., Cole, P. A., and Kuriyan, J. (2006) *Cell* **125,** 1137–1149
23. Hubbard, S. R. (2006) *Cell* **125,** 1029–1031
24. Pellicena, P., and Kuriyan, J. (2006) *Curr. Opin. Struct. Biol.* **16,** 702–709

25. Sato, T., Pallavi, P., Golebiewska, U., McLaughlin, S., and Smith, S. O. (2006) *Biochemistry* **45,** 12704–12714
26. Tebar, F., Villalonga, P., Sorkina, T., Agell, N., Sorkin, A., and Enrich, C. (2002) *Mol. Biol. Cell* **13,** 2057–2068
27. Tebar, F., Llado, A., and Enrich, C. (2002) *FEBS Lett.* **517,** 206–210
28. Holthuis, J. C., and Levine, T. P. (2005) *Nat. Rev. Mol. Cell Biol.* **6,** 209–220
29. Helmholtz, H. L. (1879) *Ann. Phys. Leipzig* **7,** 337
30. Dill, K., and Bromberg, S. (2003) *Molecular Driving Forces*, Garland Science, New York
31. McLaughlin, S. (1977) *Curr. Top. Membr. Transp.* **19,** 71–144
32. McLaughlin, S. (1989) *Annu. Rev. Biophys. Biophys. Chem.* **18,** 113–136
33. Cafiso, D., McLaughlin, A., McLaughlin, S., and Winiski, A. (1989) *Methods Enzymol.* **171,** 342–364
34. Wang, J., Arbuzova, A., Hangyas-Mihalyne, G., and McLaughlin, S. (2001) *J. Biol. Chem.* **276,** 5012–5019
35. Rusu, L., Gambhir, A., McLaughlin, S., and Radler, J. (2004) *Biophys. J.* **87,** 1044–1053
36. Golebiewska, U. P., Gambhir, A., Hangyas-Mihalyne, G., Zaitseva, I., Raedler, J., and McLaughlin, S. (2006) *Biophys. J.* **91,** 588–599
37. Buser, C. A., and McLaughlin, S. (1998) *Methods Mol. Biol.* **84,** 267–281
38. Magde, D., Elson, E. L., and Webb, W. W. (1974) *Biopolymers* **13,** 29–61
39. Maiti, S., Haupts, U., and Webb, W. W. (1997) *Proc. Natl. Acad. Sci. U. S. A.* **94,** 11753–11757
40. Sengupta, P., Balaji, J., and Maiti, S. (2002) *Methods* **27,** 374–387
41. Elson, E. L. (2004) *J. Biomed. Opt.* **9,** 857–864
42. Sorokin, A. (1995) *Oncogene* **11,** 1531–1540
43. Sorkin, A., Mazzotti, M., Sorkina, T., Scotto, L., and Beguinot, L. (1996) *J. Biol. Chem.* **271,** 13377–13384
44. Carter, R. E., and Sorkin, A. (1998) *J. Biol. Chem.* **273,** 35000–35007
45. Laemmli, U. K. (1970) *Nature* **227,** 680–685
46. Lowry, O. H., Rosebrough, N. J., Farr, A. L., and Randall, R. J. (1951) *J. Biol. Chem.* **193,** 265–275
47. Chafouleas, J. G., Bolton, W. E., Hidaka, H., Boyd, A. E., III, and Means, A. R. (1982) *Cell* **28,** 41–50
48. Nishikawa, M., and Hidaka, H. (1982) *J. Clin. Invest.* **69,** 1348–1355
49. Peitzsch, R. M., and McLaughlin, S. (1993) *Biochemistry* **32,** 10436–10443
50. McLaughlin, S., and Whitaker, M. (1988) *J. Physiol* **396,** 189–204
51. Johnson, J. D., and Wittenauer, L. A. (1983) *Biochem. J.* **211,** 473–479
52. Anfinogenova, Y. J., Rodriguez, X., Grygorczyk, R., Adragna, N. C., Lauf, P. K., Hamet, P., and Orlov, S. N. (2001) *Cell Physiol. Biochem.* **11,** 295–310
53. Aifa, S., Johansen, K., Nilsson, U. K., Liedberg, B., Lundstrom, I., and Svensson, S. P. (2002) *Cell. Signal.* **14,** 1005–1013
54. Kholodenko, B. N. (2006) *Nat. Rev. Mol. Cell Biol.* **7,** 165–176
55. Kholodenko, B. N., Demin, O. V., Moehren, G., and Hoek, J. B. (1999) *J. Biol. Chem.* **274,** 30169–30181
56. Hunter, T., Ling, N., and Cooper, J. A. (1984) *Nature* **311,** 480–483
57. Davis, R. J. (1988) *J. Biol. Chem.* **263,** 9462–9469
58. Livneh, E., Dull, T. J., Berent, E., Prywes, R., Ullrich, A., and Schlessinger, J. (1988) *Mol. Cell. Biol.* **8,** 2302–2308
59. Lund, K. A., Lazar, C. S., Chen, W. S., Walsh, B. J., Welsh, J. B., Herbst, J. J., Walton, G. M., Rosenfeld, M. G., Gill, G. N., and Wiley, H. S. (1990) *J. Biol. Chem.* **265,** 20517–20523
60. Countaway, J. L., Nairn, A. C., and Davis, R. J. (1992) *J. Biol. Chem.* **267,** 1129–1140
61. Theroux, S. J., Latour, D. A., Stanley, K., Raden, D. L., and Davis, R. J. (1992) *J. Biol. Chem.* **267,** 16620–16626
62. Feinmesser, R. L., Wicks, S. J., Taverner, C. J., and Chantry, A. (1999) *J. Biol. Chem.* **274,** 16168–16173
63. Osawa, M., Swindells, M. B., Tanikawa, J., Tanaka, T., Mase, T., Furuya, T., and Ikura, M. (1998) *J. Mol. Biol.* **276,** 165–176
64. Osawa, M., Kuwamoto, S., Izumi, Y., Yap, K. L., Ikura, M., Shibanuma, T., Yokokura, H., Hidaka, H., and Matsushima, N. (1999) *FEBS Lett.* **442,** 173–177
65. Cho, W., and Stahelin, R. V. (2005) *Annu. Rev. Biophys. Biomol. Struct.* **34,** 119–151
66. DiNitto, J. P., Cronin, T. C., and Lambright, D. G. (2003) *Sci. STKE 2003*, re16
67. Okeley, N. M., and Gelb, M. H. (2004) *J. Biol. Chem.* **279,** 21833–21840
68. Young, K. W., Willets, J. M., Parkinson, M. J., Bartlett, P., Spiegel, S., Nahorski, S. R., and Challiss, R. A. (2003) *Cell Calcium* **33,** 119–128
69. Sutherland, C. M., Moretti, P. A., Hewitt, N. M., Bagley, C. J., Vadas, M. A., and Pitson, S. M. (2006) *J. Biol. Chem.* **281,** 11693–11701
70. Stahelin, R. V., Hwang, J. H., Kim, J. H., Park, Z. Y., Johnson, K. R., Obeid, L. M., and Cho, W. (2005) *J. Biol. Chem.* **280,** 43030–43038
71. Chapin, S. J., Enrich, C., Aroeti, B., Havel, R. J., and Mostov, K. E. (1996) *J. Biol. Chem.* **271,** 1336–1342
72. Apodaca, G., Enrich, C., and Mostov, K. E. (1994) *J. Biol. Chem.* **269,** 19005–19013
73. Sheetz, M. P., and Singer, S. J. (1974) *Proc. Natl. Acad. Sci. U. S. A.* **71,** 4457–4461
74. Sheetz, M. P., and Singer, S. J. (1976) *J. Cell Biol.* **70,** 247–251
75. Chandler, W. K., Hodgkin, A. L., and Meves, H. (1965) *J. Physiol.* **180,** 821–836
76. Watanabe, H., Takahashi, R., Tran, Q. K., Takeuchi, K., Kosuge, K., Satoh, H., Uehara, A., Terada, H., Hayashi, H., Ohno, R., and Ohashi, K. (1999) *Biochem. Biophys. Res. Commun.* **265,** 697–702
77. Jan, C. R., Lu, C. H., Chen, Y. C., Cheng, J. S., Tseng, L. L., and Jun-Wen, W. (2000) *Pharmacol. Res.* **42,** 323–327
78. Schlessinger, J. (2000) *Cell* **103,** 211–225
79. Jorissen, R. N., Walker, F., Pouliot, N., Garrett, T. P., Ward, C. W., and Burgess, A. W. (2003) *Exp. Cell Res.* **284,** 31–53
80. Carpenter, G. (2000) *BioEssays* **22,** 697–707
81. Pike, L. J., Han, X., and Gross, R. W. (2005) *J. Biol. Chem.* **280,** 26796–26804
82. Hubbard, S. R. (2004) *Nat. Rev. Mol. Cell. Biol.* **5,** 464–471
83. Landau, M., Fleishman, S. J., and Ben-Tal, N. (2004) *Structure* **12,** 2265–2275
84. Aifa, S., Miled, N., Frikha, F., Aniba, M. R., Svensson, S. P., and Rebai, A. (2006) *Proteins* **62,** 1036–1043
85. Davis, R. J., Girones, N., and Faucher, M. (1988) *J. Biol. Chem.* **263,** 5373–5379
86. Hidaka, H., Yamaki, T., Naka, M., Tanaka, T., Hayashi, H., and Kobayashi, R. (1980) *Mol. Pharmacol.* **17,** 66–72
87. Molecular Probes, Inc. (XXXX) *Conjugation with Thiol-reactive Probes*, Molecular Probes, Inc., Eugene, OR